Journal of Applied Analysis and Computation
Volume 12, Number 5, October 2022, 1748–1762
Website:http://www.jaac-online.com
DOI:10.11948/20210269

THE EFFECTIVENESS OF HUMAN INTERVENTIONS AGAINST COVID-19 BASED ON EVOLUTIONARY GAME THEORY*

Susu Jia[1], Xinzhu Meng[1,†] and Tonghua Zhang[2]

Abstract Social distancing strategy (including Six-Foot Rule, wearing masks, and other easy-to-operate measures) and quarantine measures have played a critical role in the early stage of the COVID-19 epidemic. In order to explore the mechanisms of these two human interventions accurately, we develop a coupling epidemiological-behavioral model based on evolutionary game theory. Individuals decide whether to take strategy measures based on rational consideration of payoffs. Moreover, authorities also balance the costs and effectiveness of the interventions at the public level. Our simulation shows that social distancing strategy can suppress every single outbreak effectively. In the early stage of an epidemic, the implementation of the quarantine measures determines the scale of the epidemic. Timely and effective quarantine measures can control recurrent outbreaks without social lockdown. Support policy for individual-level intervention or high diagnosis rates are beneficial to control the epidemic but require long-term social lockdown.

Keywords COVID-19, mathematical epidemiology, imitation dynamics, quarantine, social distancing.

MSC(2010) 91A22, 92B05.

1. Introduction

COVID-19, the serious respiratory infectious disease caused by the new type virus SARS-CoV-2, its rapid spread have done great harm to people's life and social stability. As of 31 December 2020, about 103.4 million people worldwide have benn diagnosed [8]. Even in a developed country with world-class health care, the daily increase in confirmed cases is up to 200 thousand [8]. COVID-19 pandemic was not immediately suppressed, and the second wave occurred in October 2020 [5,14]. It is essential to develop a sustainable control methods for the early stages of new epidemics [20,32].

†The corresponding author. Email: mxz721106@sdust.edu.cn(X. Meng)
1College of Mathematics and Systems Science, Shandong University of Science and Technology, Qianwan'gang Rode, 266590 Qingdao, China
2Department of Mathematics, Swinburne University of Technology, Hawthorn, Victoria 3122, Australia
*This work was supported by the SDUST Research Fund (2014TDJH102), the Research Fund for the Taishan Scholar Project of Shandong Province of China, Shandong Provincial Natural Science Foundation of China (ZR2019MA003), and the SDUST Innovation Fund for Graduate Students (YC20210255).

Since people infected with SARS-CoV-2 have an incubation period, most of the research is an extension of the classical $SEIR$ model [18, 21, 22, 34]. Taking population migration into account, Yang etc [34] used the $SEIR$ model and epidemiological data from the first two months of COVID-19 to describe the epidemic, and used an AI method to predict trends, which was trained on SARS data from 2003. And Liu etc [22] developed two $SEIRU$ models to delve deeper into exposure or incubation period, one of which had time delay. Lei [17] established a difference equation model and well predicted the changes in the recent confirmed cases of infectious diseases such as COVID-19.

There are three modes of transmission of COVID-19, namely direct transmission, aerosols transmission and contact transmission. There is now compelling evidence that covid-19 is mainly transmitted via airborne respiratory aerosols. Because pathogen-bearing aerosol droplets are small enough to mix well indoors, only Six-Foot Rule of social distancing dose not provide effective protection. Wearing face masks is the most effective method to prevent interhuman transmission [10, 11, 16, 20]. Combined wearing masks with Six-Foot Rule, quarantine and contact tracing, the social distancing strategy will most likely stop the COVID-19 pandemic [36]. Thereby, the so-called "social distancing strategy" in this investigation includes those easy-to-operate individual epidemic prevention measures, such as wearing masks, timely disinfection, and reducing exposure. But reducing going out and Six-Foot Rule affect people's normal lives. Especially when the scope is expanded to the whol pipulation, the Great Lockdown is formed. It will inevitably bring about additional consumption and obstacles to economic and social development. In fact, the Great Lockdown has a negative impact on economic growth [23, 26]. In terms of mental health, people having long-term indoor life will have negative mentality and may rise depressive psychological problems [24, 28, 30].

In fact, the state of population epidemic prevention behavior will affect epidemiological dynamics. Evolutionary game theory (EGT) has been used to study the impact of individual epidemic prevention behavior epidemiology. Individuals make behavior decisions by measuring the income difference of different epidemic prevention strategies. In addition, personal experience and the speed of reaction to relevant information are also very important to the game [29].

The investigations of coupling epidemic-behavior are generally based on two different kinds of assumptions: modeling on well mixed homogenous populations, or networks [6]. The former highlights individual perceptions of benefits, while the latter focuses on reflecting the impact of demographic structure. Based on the EGT framework in well-mixed populations, Piero etc [28] modeled behavioral changes through an imitation process with the consideration of perceived prevalence of infections and effects of misconception of risk. In this study, asymptomatic infected individuals and recovery individuals also participated in the game. Exposed cases have the same decision-making process as susceptible individuals, and their behavior will deeply affect the epidemiological dynamics. Their investigation highlights that imitation can not change their epidemical status. Li etc [19] applied the network method to study how the the behavior of weak a mask affect a pandemic. Amaral etc [1] highlighted the critical role of social strategies on COVID-19. In addition, Kabir etc [13] had even floated the idea of balancing costs in the economic field.

The quarantine we consider is not individual home quarantine, but the strict and effective epidemic prevention measures guaranteed by public health institutions. They quarantine contagious cases to specific sites and investigate their epidemiological history in detail, looking for sources of infection and potential infections. Xu etc [33] proved that the quarantine of close contacts has significant effect on reducing the number of daily new cases. This measure is more effective than home quarantine and can detect incubation patients as early as possible [12, 20, 33, 35]. Such public interventions to curb COVID-19 have had varying degrees of success in countries [10, 16, 25]. Boulfoul etc [4] demonstrated the key role of quarantine in disease clearance through an epidemic model.

In order to investigate human interventions in the early stage of COVID-19, we propose a coupling epidemiological-behavioral model in Section 2 and present the main results of numerical simulation in Section 3. The final section is the discussion and conclusions.

2. Model and Assumptions

2.1. Epidemiological model

COVID-19 has an incubation period, and the incubation period cases are contagious. We divide the population into five compartments – susceptible (S), exposed (E), symptomatic (I), quarantine (Q), recoverd (R). Our investigation focus on the early stage of the pandemic and therefore do not consider population dynamics such as natural birth-death and migration over a short period of time. It is assumed that the total population $N(t)$ satisfies $N(t) = S(t) + E(t) + I(t) + Q(t) + R(t) = 1$, i.e. the above variables all represent the proportion of each state in the total population. Based on the above assumptions, we establish the $SEIQR$ epidemic model:

$$\begin{cases} \dot{S}(t) = -(\beta_{_I} I + \beta_{_E} E)S, \\ \dot{E}(t) = (\beta_{_I} I + \beta_{_E} E)S - \theta E, \\ \dot{I}(t) = \alpha E - \zeta I, \\ \dot{Q}(t) = q_1 E + q_2 I - \gamma_2 Q, \\ \dot{R}(t) = \gamma_0 E + \gamma_1 I + \gamma_2 Q, \end{cases} \tag{2.1}$$

where $\theta = \alpha + \gamma_0 + q_1$ and $\zeta = q_2 + \gamma_1$. The detailed comments and value ranges all parameters are shown in Table 1.

By the next generation matrix approach [31], the basic reproductive number of model (2.1) is $\hat{R}_0 = \frac{B}{\theta}$, where $B = \beta_{_E} + \frac{\alpha}{\zeta}\beta_{_I}$.

2.2. Imitation process

We assume that the imitation of epidemic prevention behavior occurs in a well-mixed population. Some of the exposed individuals may be self-healing, that is, enter $R(t)$ directly from $E(t)$, and the exposed individuals and recovery individuals will still make decisions about epidemic prevention behaviors psychologically. So we have three classes of participants, including susceptible, exposed, and recovering classes.

According to the individual's willingness to prevent epidemic, the individual's epidemic prevention strategy is devided into positive strategy C and the negative strategy D. It is a two-strategy game, cooperation and defection, similar to the prisoner's dilemma. The positive one can reduce the risk of infection for individuals,

Table 1. Epidemiology and imitation process parameters

parameters	Description	Range	Baseline	Source
γ_i	The removement rates from infected compartments	$[0.072, 0.238]$	0.154	[34]
β_E	Transmission rate for exposed individuals	$[0.152, 0.163]$	0.157	[34]
β_I	Transmission rate for symptomatic individuals	$[0.760, 0.814]$	0.787	[34]
$1/\alpha$	The average duration of incubation	$[4.1, 7.0]$	5.2	[34]
q_1	The quarantine rate of E	$[0, 1]$	0.11	-
q_2	The quarantine rate of I	$[0, 1]$	0.7	-
σ	relative risk of infection	$[0.13, 0.87]$	0.33	[27]
ρ	Speed of the behavioral changes	$[10^{-3}, 10^3]$	925	-
c	The investment in social distancing strategy per unit time	$[0, 10^3]$	0.001	-
μ	Rate of the irrational exploration	$[0, 1]$	10^{-8}	[29]

but at an additional cost. When individuals with different strategies meet, they will rationally compare the expected payoffs of the two to decide whether to imitate the behavior of the other [2].

The modeling approach of imitation dynamics of a 2-strategy game has been widely recognized. It can be described as

$$\dot{x}(t) = x(1-x)\Delta\pi + \mu(1-x) - \mu x, \tag{2.2}$$

where x is the fractions of one strategy, $1-x$ is anothor one's, and μ is the irrational decisions which avoids the undesirable effect of strict imitation [29].

According to the hypothesis, the players are divided into six substates: S_D, E_D, R_D, S_C, E_C, R_C. Let $P(t) = P(t)$ as the total players, and $P_C(t) = S_C(t)+E_C(t)+R_C(t)$ as the strategy C players, $P_D(t) = S_D(t) + E_D(t) + R_D(t)$ as the strategy D players. According to (2.2), the imitation dynamics model is established:

$$\begin{cases} \dot{S_D}(\tau) = \Delta\pi[S_C P_D \mathcal{H}(\Delta\pi) + S_D P_C \mathcal{H}(-\Delta\pi)] + \mu(S_C - S_D), \\ \dot{S_C}(\tau) = -\Delta\pi[S_C P_D \mathcal{H}(\Delta\pi) + S_D P_C \mathcal{H}(-\Delta\pi)] - \mu(S_C - S_D), \\ \dot{E_D}(\tau) = \Delta\pi[E_C P_D \mathcal{H}(\Delta\pi) + E_D P_C \mathcal{H}(-\Delta\pi)] + \mu(E_C - E_D), \\ \dot{E_C}(\tau) = -\Delta\pi[E_C P_D \mathcal{H}(\Delta\pi) + E_D P_C \mathcal{H}(-\Delta\pi)] - \mu(E_C - E_D), \\ \dot{R_D}(\tau) = \Delta\pi[R_C P_D \mathcal{H}(\Delta\pi) + R_D P_C \mathcal{H}(-\Delta\pi)] + \mu(R_C - R_D), \\ \dot{R_C}(\tau) = -\Delta\pi[R_C P_D \mathcal{H}(\Delta\pi) + R_D P_C \mathcal{H}(-\Delta\pi)] - \mu(R_C - R_D), \end{cases} \tag{2.3}$$

where $\mathcal{H}(\cdot)$ is the Heaviside function:

$$\mathcal{H}(x) = \begin{cases} 1, & x \geqslant 0, \\ 0, & x < 0. \end{cases} \tag{2.4}$$

The information available to players is confirmed cases. In model (2.1), we assume that $Q(t)$ is the confirmed case in quarantine, so the infection risk is expressed as the proportion of confirmed cases $Q(t)$. Assuming that the cost of strategy C is c, the reduction coefficient of infection risk is $\sigma(0 < \sigma < 1)$. strategy D has no cost, and is at full risk of infection. Therefore, the payoff functions of two strategies are :$\pi_D = -Q(t)$, $\pi_C = -c - \sigma Q(t)$. When encountering players with different strategy, the individual changes behavior with a proportional to the difference in the payoff function

$$\begin{aligned}\Delta\pi &= \pi_D - \pi_C \\ &= c - (1-\sigma)Q.\end{aligned} \tag{2.5}$$

Let $\Delta\pi = 0$, there is a threshold $m = \frac{c}{1-\sigma}$ of the infection risk. If it reaches the threshold, players will tend to imitate strategy C since $\pi_D < \pi_C$; On the contrary, players will prefer strategy D when the infection risk gets lower than the threshold.

2.3. Coupled system

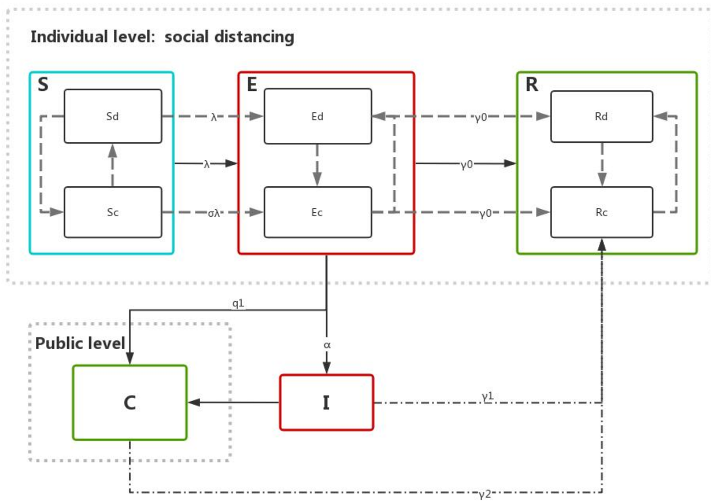

Figure 1. The epidemic flow between epidemiological classes (represented by solid black lines) and imitation flow between strategy classes (represented by gray dotted lines).

In order to the proportion of prevention strategies, we defined x as the proportion of susceptible strategy D in total players, y as the proportion of exposed players using strategy D in total players, and z as the proportion of strategy C in total players. :

$$x = \frac{S_D(t)}{P(t)}, \quad y = \frac{E_D(t)}{P(t)}, \quad z = \frac{P_C(t)}{P(t)},$$

then we have

$$S_D = xP, \quad S_C = S - xP, \quad E_D = yP, \quad E_C = E - yP.$$

In particular, the imitation process is under different time scale against epidemic transmission (τ instead of t). In this investigation, we assume $\tau = \rho t$. Here, ρ is the difference between the speed of information dissemination required for decision-making and virus dissemination. In the imitation process, rational decision-making occurs when two strategies encounter while the irrational part may occur at any time. Under the time scale of epidemical transmission, the rational part of imitation dynamics requires multiplying by ρ. Then we have the coupling model:

$$\begin{cases} \dot{S}(t) = -\lambda\left[\sigma S + xP(1-\sigma)\right], \\ \dot{E}(t) = \lambda\left[\sigma S + xP(1-\sigma)\right] - \theta E, \\ \dot{I}(t) = \alpha E - \zeta I, \\ \dot{Q}(t) = q_1 E + q_2 I - \gamma_2 Q, \\ \dot{R}(t) = \gamma_0 E + \gamma_1 I + \gamma_2 Q, \\ \dot{x}(t) = -x\lambda - x\dfrac{P'}{P} + \rho\mu(\dfrac{S}{P} - 2x) + \rho\Delta\pi\left[xzP + [S(1-z) - xP]\mathcal{H}(\Delta\pi)\right], \\ \dot{y}(t) = x\lambda - \theta y - y\dfrac{P'}{P} + \rho\mu(\dfrac{E}{P} - 2y) + \rho\Delta\pi\left[yzP + [E(1-z) - yP]\mathcal{H}(\Delta\pi)\right], \\ \dot{z}(t) = (1-z)\dfrac{P'}{P} + y(\alpha + q_1) - \rho\left[z(1-z)P\Delta\pi - \mu(1-2z)\right], \end{cases} \tag{2.6}$$

where $P' = -(\alpha + q_2)E + \gamma_1 I + \gamma_2 Q$ and $\lambda = \beta_I I + \sigma\beta_E E + (1-\sigma)\beta_E yP$. All variables and parameters are positive for all $t \geqslant 0$. Its feasible region is $D = \left\{(S, E, I, Q, R, x, y, z) \in R_+^8 | S + E + I + Q + R = 1, x + y + z \leqslant 1\right\}$. Figure 1 is the flow chart of the coupling model.

The disease-free equilibrium of system (2.6) is

$$(1, 0, 0, 0, 0, \frac{c + \sqrt{c^2 + 4\mu^2}}{c + 2\mu + \sqrt{c^2 + 4\mu^2}}, 0, \frac{c + 2\mu - \sqrt{c^2 + 4\mu^2}}{2c}),$$

and the basic reproductive number is $R_0 = [\sigma + (1-\sigma)x]\hat{R}_0 = \kappa\hat{R}_0$. Coupled to model (2.3), a decay coefficient κ is multiplied by the basic reproductive number of model (2.1). And the coefficient is determined by the protection efficiency σ of strategy C and x_0, where

$$x_0 = \frac{c + \sqrt{c^2 + 4\mu^2}}{c + 2\mu + \sqrt{c^2 + 4\mu^2}}.$$

Letting $q_i = 0, i = 1, 2$ will get the basic representative number in the scenario without quarantine.

3. Simulations and Result

Initial conditions

The epidemiological parameters in the numerical simulation in this investigation are taken from the literature [34]. At the start of the outbreak, most people adopt strategy D. And we assume that the irrational factor is a small constant. Other initial conditions are listed in Table 2.

Baseline scenario

To measure the effect and cost of epidemic prevention deployment in a certain area, it is necessary to set relevant indicators in the simulation: the final size of infection (FIS), the peak of confirmed cases (C-peak), the peak of actual infection (A-peak),

Table 2. Model variables and initial conditions

Variabs	S	E	I	Q	R	x	y	z
Initial values	$1-10^{-4}$	8×10^{-5}	2×10^{-5}	0	0	$\frac{(1-10^{-6})\times(1-10^{-4})}{1-2\times10^{-5}}$	$\frac{(1-10^{-6})\times8\times10^{-5}}{1-2\times10^{-5}}$	10^{-6}

the percentage of the big lockdown (more than half people adopt strategy C, i.e. the duration of $z > 0.5$) in 400 days (Lockdown), the cost of infection (Infection) and the relative cost of human interventions (Interventions).

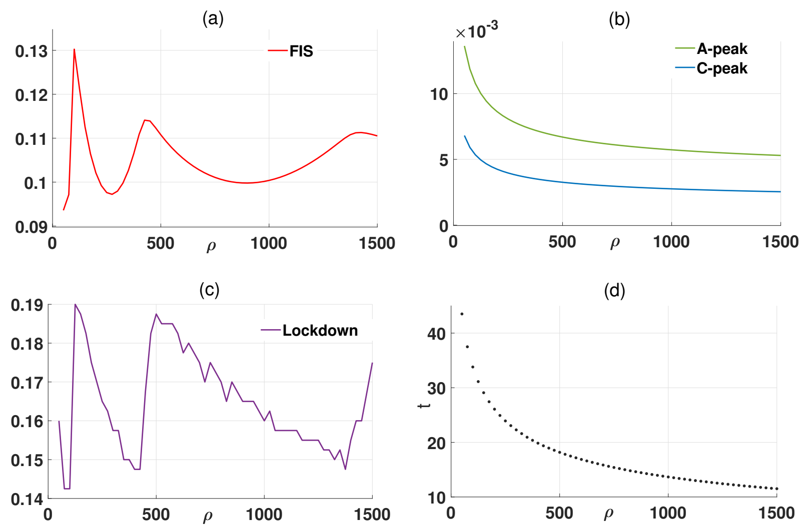

Figure 2. Imitation speed ρ sequence plots of each index. (a) The value of FIS with imitation speed axis ρ. (b) The value of A-peak and C-peak with imitation speed axis ρ. (c). The value of Lockdown with imitation speed axis ρ. (d). The scatter of delay with imitation speed axis ρ.

Consider different relative imitation speeds ρ to conduct the first simulation. The simulation results of the four indicators are summarized in Fig. 2. It shows that peak values and behavior delay both decrease monotonically with the increase ρ, while FIS and Lockdown show non-monotonic change. For the generality of results, exclude the value of ρ that makes FIS and Lockdown extreme.

When the proportion of existing confirmed cases $Q(t)$ reaches the threshold m, the individual responds. However, due to the difference in the speed of imitation, individuals are delayed in their response. According to the scatter plot of confirmed cases in Beijing and Liaoning province at the beginning of the epidemic (see Fig. 3), the duration of a single outbreak is about 15 to 25 days, and it takes about 14 days for more than half of the population to respond to the epidemic. According to the Fig. 2(d), Delay=14 corresponds to $\rho = 925$, and the FIS and Lockdown at this time are not extreme values.

Therefore, the parameters of the baseline scenario are determined, and its time series diagrams of confirmed cases and strategies are shown in Fig. 4(a). The trend of confirmed cases in numerical simulation is consistent with that of actual confirmed cases in Fig. 3, so the parameter setting of baseline scenario is of practical significance. And the time series plots of the no-quarantine baseline scenario are plotted

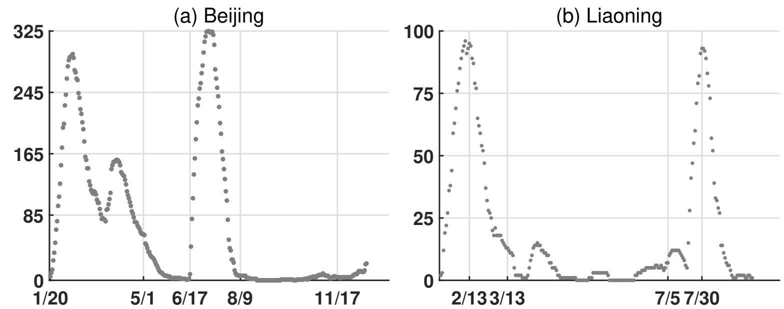

Figure 3. The time series plots of COVID-19 confirmed cases in Beijing and Liaoning province.

as a control group in Fig. 4(b). The comparison of the time series plots shows that under the baseline scenario, the duration of the first wave in no-quarantine scenario is longer, with a larger proportion of confirmed cases $Q(t)$ and a longer duration of big Lockdown. A further comparison of the indicators of the quarantine, as well as the scenario with a higher diagnosis rate, are plotted in Fig. 4(c) and Fig. 4(d).

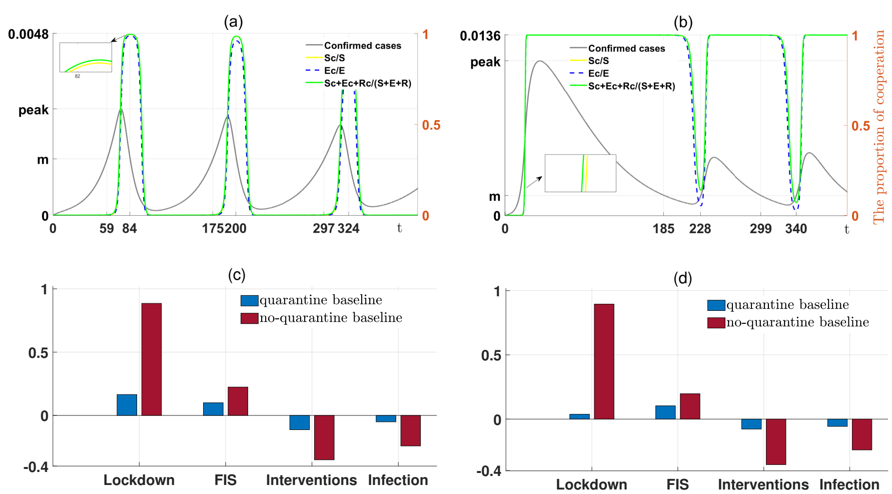

Figure 4. Comparative simulation of quarantine measures. (a) The baseline scenario with quarantine. (b) The baseline scenario without quarantine. (c) Bar comparison chart of baseline scenario indicators on quarantine measures. (d). Bar comparison of indicators on quarantine measures at a higher diagnosis rate.

About 78 days after the first wave ended, the outbreak resurfaces. And the values of the subsequent outbreaks are lower than those of the first wave. In the first wave, the proportion of confirmed cases $Q(t) > m$ for 25 days and the population response is delayed by 14 days. We call the situation where $z > 0.5$ social lockdown. And confirmed cases alse peaks after half a day of it occures. As can be seen from Fig. 4(a), the proportion of cooperative players of susceptibles $\frac{S_C}{S}$ is almost equal to the proportion of cooperative players of all players. The proportion of cooperative players of exposed cases is slightly lower, which has little effct on the proportion of total cooperative players.

Under the same conditions, the value of the index Lockdown of the scenario without quarantine is much larger, which has more outbreaks. In addition, the value of index C-peak is 3.7 times higher than the scenario with quarantine, and the curve drops slowly after reaching the peak. That is, each outbreak lasts longer. But the reaction of population is faster. Without public-level measures, individuals are more susceptible to epidemic prevention.

Under baseline scenario, the ratio of A-peak to C-peak is 2.07 with quarantine and 1.93 without quarantine. The value of A-peak without quarantine is 2.88 times higher than with quarantine, and the value of C-peak is 3.15 times higher. Under the same circumstances, the baseline scenario with quarantine has fewer outbreaks, and the accompanying social distancing strategy lasts for a shorter period. Meanwhile, the values of index FIS and costs are lower.

Set higher diagnosises, the ratio of A-peak to C-peak in the scenario with quarantine decreases to 1.84, and the same value in the scenario without quarantine decreases to 1.82. The diagnosis rates q_1 and q_2 determines the gap between the two peaks. In the scenario without quarantine measures, epidemic control relies on prolonged social lockdown, and the effct is not as effective as that in the case of quarantine measures.

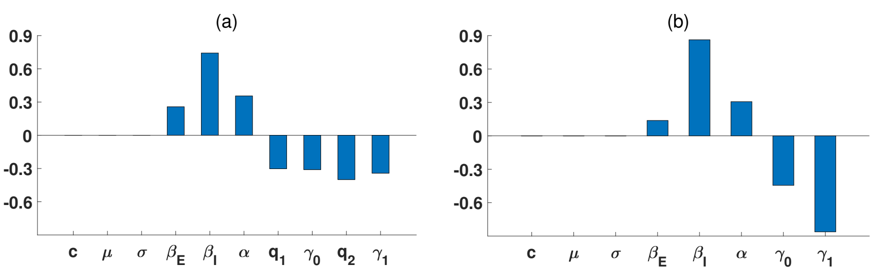

Figure 5. The sensitivity analysis of R_0 in baseline scenarios. (a) The sensitivity analysis of the scenario with quarantine measures. (b) The sensitivity analysis of the scenario without quarantine measures.

Calculate the normalized forward sensitivity indices of R_0 with resoect to each parameters, and the reluts are shown in Fig. 5(a). And the same sensitivity index analysis is done for the model without quarantine, and the results are shown in Fig. 5(b). The value of every bar indicates the change of R_0 caused by 1% increase of each parameter. For example, 1% increase of α will cause the 40% increase of R_0, meanwhile 1% increase of q_2 will decrease R_0 by 40%. And the increase of imitation parameters will not significantly affect R_0 in the baseline scenario. Thereby, for curbing the pandemic, increasing the recovery rate and the diagnosis rate is the directions of efforts. That is, the quarantine is the key of controlling the infection scale.

Simulations of ξ

We assume the relative risk of infection is proportional to the investment ($\sigma \propto \frac{1}{c}$). With the increase of investment c, the prevention effect of strategy C is better, i.e. the smaller σ. It is reasonable to assume the reduction factor is the hyperbolic function of the additional cost c: $\sigma(c) = \frac{1}{1+\xi c}$ [3]. There are only two cases of investment in our investigation: 0 or fixed constant c, corresponding to strategy D

and strategy C, respectively. Furthermore, ξ indicates the impact of local authorities on individual-level intervention. Higher ξ indicates the support policy of the authority to individuals. Therefore, individuals can get better results with the same investment. In simulation III, we first compare the baseline scenario with the negative policy $\xi^1 = 0.5\xi^0$ and the support policy $\xi^2 = 1.5\xi^0$ respectively. In the former case, players still invest in the same cost as the baseline but bear the higher risk $\sigma = 0.5$; Meanwhile, in the latter case, bear the lower risk $\sigma = 0.25$ under the same cost. The result is shown in Fig. 6. Considering the the scenario with quarantine measures, the percentage changes of the epidemic prevention indices of ξ^1 and ξ^2 compared with ξ^0 are shown in Fig. 6(a). Support policy and quarantine measures are both public-level intervention. To compare their epidemic prevention effects, scenario one has quarantine measures but with ξ^2, and scenario two is ξ^1 without quarantine measures. The percentage changes of epidemic prevention indices compared with the no-quarantine baseline scenario are summarized in Fig. 6(b).

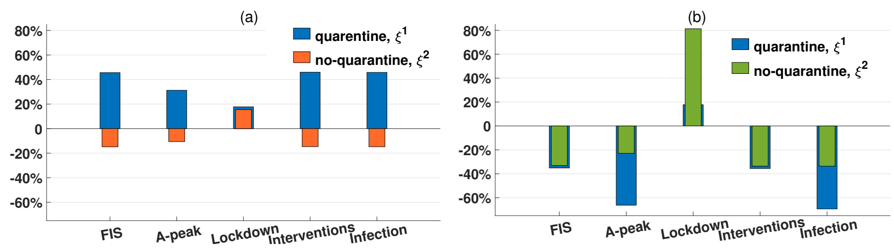

Figure 6. Percentage of changes of epidemic prevention indicators of support policy. (a) The effectiveness of support policy. (b) The comparison between quarantine and support policies quarantine. Percentage of changes in epidemic prevention indies of support policy.

Compared to the baseline scenario, the support policy can reduce the FIS and peak values. With the support policy, individual protection is more effective, and the epidemic is well controlled based on 15% longer social lockdown duration. The relative cost of human interventions falls by 14.6% from the baseline. In scenario with quarantine measures, whether the authorities support individuals or not, the duration of social lockdown will increase. However, supporting individuals can effectively reduce the consumption of total cost of interventions.

In scenario without quarantine measures, which one is a more worthwhile public-level intervention? The figure 6(b) indicates that quarantine is more worthwhile. Support policy for individuals without quarantine measures will greatly increase the duration of social lockdown, which is not an ideal situation.

The interaction between two levels of human interventions

To further explore the interaction between the two levels of human interventions, we design the following simulation, and the result is given in Fig. 7:

1. The interaction of diagnosis rates q_1 and q_2 and the interaction between imitation speed ρ and diagnosis rate q_2 in the system (2.6) (Fig. 7(a));
2. The interaction of diagnosis rates q_1 and q_2 and the interaction between imitation speed ρ and diagnosis rate q_2 in the Non-Isolation system (Fig. 7(b)).

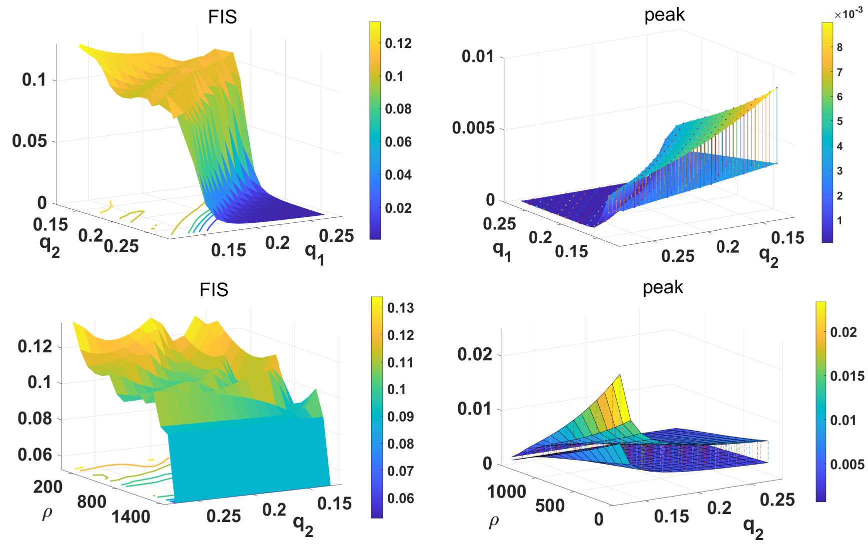

(a)

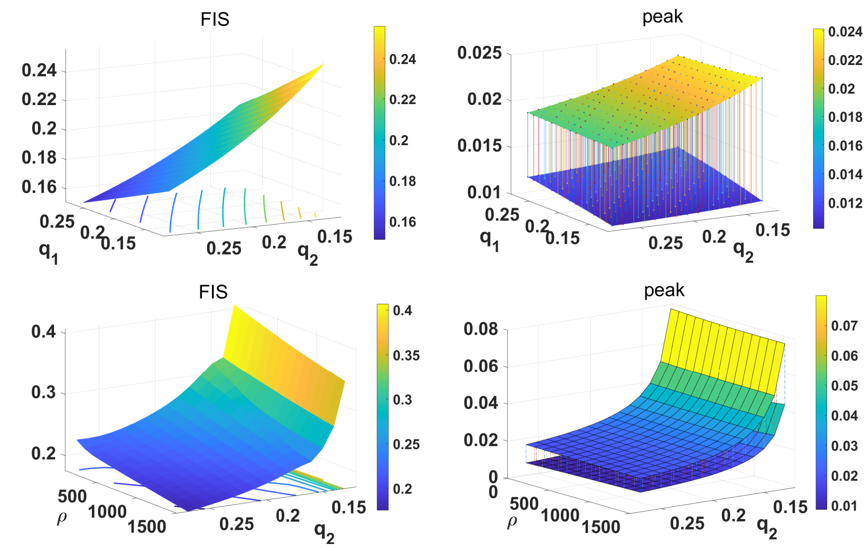

(b)

Figure 7. Simulation of interaction between two levels of human interventions. (a) The FIS and two peaks in the scenario with quarantine measures. (b) The FIS and the two peak values in the scenario without quarantine measures. $q_1 \in (0.13, 0.27)$, $q_2 \in (0.13, 0.27)$ and $\rho \in (50, 1500)$, and other parameters of the baseline scenario are reported in Table 1.

When individual decision-making is slow, the infection scale is highly sensitive to the quarantine rate. Increasing quarantine rate can effectively control the size of a single outbreak, but the influence on the final infection scale is not monotonous. When the individual responds quickly, the scale of infection is determined by the relationship between the diagnosis rate q_i. When q_i satisfies $q_1 > 0.4 - q_2$, both FIS and peak value can be well controlled.

The plot of peak indicates that the intensity of the quarantine directly affects the size of every single outbreak. If enhance the intensity of quarantine measures, the confirmed patient data will be closer to the actual disease data. In scenario without quarantine measures, increasing the diagnosis rates directly increases the individual's perceived risk of infection, so the control effect depends on higher Lockdown.

Fixed the value of q_1, we focus on the relationship between q_2 and imitation speed ρ. In scenario with quarantine measures (Fig. 7(a)), faster imitation can reduce the number of outbreaks when q_2 is small. However, in the areas with high q_2, the increase of ρ has no significant effect on the peak value. In the scenario without quarantine measures, the diagnosis rate is the dominant factor (Fig. 7(b)). In this case, the interventions at the individual level can only play a weak role.

4. Discussion and Conclusions

Early prevention measures are essential for the outbreak of new infectious diseases. In this paper, we extend the model already introduced in [27] and establish the coupled epidemiological-behavioral model, to investigate the human interventions of epidemic prevention at individual and public levels. Those cooperative exposed cases can help curbing disease transmission by reducing the spread of the virus. Our investigation emphasizes that spontaneous behavioral change can buy enough time for further medical research. Nevertheless, the faster individual imitation reaction speed will lead to more small-scale outbreaks. Furthermore, appropriate speed of imitation can reduce the daily prevalence of infection [15] and the eventual epidemic [7, 9].

Relying on the Big Lockdown is not reliable, because of its unavoidable negative effects. Therefore, the public-level interventions are necessary. Our result shows that the intensity of separate quarantine determines the scale of the epidemic. In the areas without quarantine interventions, high diagnosis rates or support policies for individual measures can help epidemic control, but the impact is modest and limited.

In addition, our investigation has noticed that if the irrational factors of individual decision-making are high, the proportion of each strategy tends to be equal. In this case, disease control will be more difficult. It is crucial to conduct scientific education in time to guide the public to view the epidemic scientifically and make rational decisions.

Declaration of Interests

The authors declare that they have no known competing financial interests or personal relationships that could have influenced the work reported in this paper.

Acknowledgements

This work was supported by the SDUST Research Fund (2014TDJH102), the Research Fund for the Taishan Scholar Project of Shandong Province of China, Shandong Provincial Natural Science Foundation of China (ZR2019MA003), and the SDUST Innovation Fund for Graduate Students (YC20210255).

References

[1] M. A. Amaral, M. M. de Oliveira and M. A. Javarone, *An epidemiological model with voluntary quarantine strategies governed by evolutionary game dynamics*, arXiv[physics.soc-ph], 2020, 13–15.

[2] C. T. Bauch, *Imitation dynamics predict vaccinating behaviour*, Proc. Biol. Sci., 2005, 272(1573), 1669–1675.

[3] S. Bhattacharyya and T. Reluga, *Game dynamic model of social distancing while cost of infection varies with epidemic burden*, IMA Journal of Applied Mathematics, 2019, 84(1), 23–43.

[4] B. Boulfoul, A. Kerboua and X. Zhou, *Mathematical modeling and analysis of an epidemic model with quarantine, latent and media coverage*, Journal of Nonlinear Modeling and Analysis, 2022, 4(1), 43–63.

[5] G. Cacciapaglia, C. Cot and F. Sannino, *Second wave Covid-19 pandemics in europe: a temporal playbook*, Sci. Rep., 2020, 10(1), 15514.

[6] S. Chang, M. Piraveenan, P. Pattison et al., *Game theoretic modelling of infectious disease dynamics and intervention methods: a review*, J. Biol. Dyn., 2020, 14(1), 57–89.

[7] S. Del Valle, H. Hethcote, J. M. Hyman et al., *Effects of behavioral changes in a smallpox attack model*, Math. Biosci., 2005, 195(2), 228–51.

[8] E. Dong, H. Du and L. Gardner, *An interactive web-based dashboard to track Covid-19 in real time*, Lancet. Infect. Dis., 2020, 20(5), 533–534.

[9] S. Funk, E. Gilad, C. Watkins et al., *The spread of awareness and its impact on epidemic outbreaks*, Proc. Natl. Acad. Sci., 2009, 106(16), 6872–6877.

[10] L. P. Garcia and E. Duarte, *Nonpharmaceutical interventions for tackling the Covid-19 epidemic in Brazil*, Epidemiol. Serv. Saude., 2020, 29(2), e2020222.

[11] S. Hanaei and N. Rezaei, *Covid-19: Developing from an outbreak to a pandemic*, Arch. Med. Res., 2020, 51(6), 582–584.

[12] J. Hellewell, S. Abbott, A. Gimma et al., *Feasibility of controlling Covid-19 outbreaks by isolation of cases and contacts*, Lancet. Glob. Health., 2020, 8(4), e488–e496.

[13] K. M. A. Kabir and J. Tanimoto, *Evolutionary game theory modelling to represent the behavioural dynamics of economic shutdowns and shield immunity in the Covid-19 pandemic*, R. Soc. Open. Sci., 2020, 7(9), 201095.

[14] A. K. Kaliya-Perumal, J. Kharlukhi and U. F. Omar, *The second wave of Covid-19: time to think of strategic stockpiles*, Can. J. Public. Health., 2020, 111(4), 486–487.

[15] I. Z. Kiss, J. Cassell, M. Recker et al., *The impact of information transmission on epidemic outbreaks*, Math. Biosci., 2010, 225(1), 1–10.

[16] M. U. G. Kraemer, C. Yang, B. Gutierrez et al., *The effect of human mobility and control measures on the Covid-19 epidemic in China*, Science, 2020, 368(6490), 493–497.

[17] C. Lei and X. Han, *Regional prediction of Covid-19 in the United States based on the difference equation model*, Journal of Nonlinear Modeling and Analysis, 2021, 3(4), 547–559.

[18] Q. Li, X. Guan, P. Wu et al., *Early transmission dynamics in Wuhan, China, of novel coronavirus-infected pneumonia*, N. Engl. J. Med., 2020, 382(13), 1199–1207.

[19] W. Li, J. Zhou and J. Lu, *The effect of behavior of wearing masks on epidemic dynamics*, Nonlinear Dyn., 2020, 101(3), 1–7.

[20] Y. Li, R. Zhang, J. Zhao et al., *Understanding transmission and intervention for the Covid-19 pandemic in the United States*, Sci. Total. Environ., 2020, 748, 141560.

[21] Y. Liu, A. A. Gayle, A. Wilder-Smith et al., *The reproductive number of Covid-19 is higher compared to SARS coronavirus*, J. Travel Med., 2020, 27(2), 1–4.

[22] Z. Liu, P. Magal, O. Seydi et al., *A covid-19 epidemic model with latency period*, Infect. Dis. Model, 2020, 5(11811530272), 323–337.

[23] International Monetary Fund, *World Economic Outlook: A Long and Difficult Ascent*, Report 9781513556055, International Monetary Fund, 2020.

[24] M. G. Mazza, R. De Lorenzo, C. Conte et al., *Anxiety and depression in Covid-19 survivors: Role of inflammatory and clinical predictors*, Brain Behav. Immun., 2020, 89, 594–600.

[25] K. Meier, T. Glatz, M. C. Guijt et al., *Public perspectives on protective measures during the Covid-19 pandemic in the Netherlands, Germany and Italy: A survey study*, PLoS One, 2020, 15(8), e0236917.

[26] E. Otte Im Kampe, A. S. Lehfeld, S. Buda et al., *Surveillance of Covid-19 school outbreaks, Germany, march to August 2020*, Euro. Surveill, 2020, 25(38), 2001645–2001645.

[27] P. Poletti, M. Ajelli and S. Merler, *The effect of risk perception on the 2009 h1n1 pandemic influenza dynamics*, PLoS One, 2011, 6(2), e16460.

[28] P. Poletti, M. Ajelli and S. Merler, *Risk perception and effectiveness of uncoordinated behavioral responses in an emerging epidemic*, Math. Biosci., 2012, 238(2), 80–89.

[29] P. Poletti, B. Caprile, M. Ajelli et al., *Spontaneous behavioural changes in response to epidemics*, J. Theor. Biol., 2009, 260(1), 31–40.

[30] N. Salari, A. Hosseinian-Far, R. Jalali et al., *Prevalence of stress, anxiety, depression among the general population during the Covid-19 pandemic: a systematic review and meta-analysis*, Global Health, 2020, 16(1), 57.

[31] P. van den Driessche and J. Watmough, *Reproduction numbers and sub-threshold endemic equilibria for compartmental models of disease transmission*, Math. Biosci., 2002, 180(1-2), 29–48.

[32] G. Wallentin, D. Kaziyeva and E. Reibersdorfer-Adelsberger, *Covid-19 intervention scenarios for a long-term disease management*, Int. J. Health Policy Manag, 2020, 9(12), 508–516.

[33] C. Xu, Z. Zhang, X. Huang et al., *The dynamic effects of different quarantine measures on the spread of Covid-19*, Journal of Applied Analysis and Computation, 2022, 1–1.

[34] Z. Yang, Z. Zeng, K. Wang et al., *Modified seir and ai prediction of the epidemics trend of Covid-19 in China under public health interventions*, J. Thorac. Dis., 2020, 12(3), 165–174.

[35] N. Zhang, P. Cheng, W. Jia et al., *Impact of intervention methods on Covid-19 transmission in Shenzhen*, Build. Environ., 2020, 180, 107106.

[36] R. Zhang, Y. Li, L. Zhang et al., *Identifying airborne transmission as the dominant route for the spread of Covid-19*, Proceedings of the National Academy of Sciences, 2020, 117(26), 14857–14863.